The flavoheme reductase Ncb5or protects cells against endoplasmic reticulum stress-induced lipotoxicity[S]

Yongzhao Zhang,[1,*] Kevin Larade,[1,*] Zhi-gang Jiang,[*] Susumu Ito,[†] WenFang Wang,[§] Hao Zhu,[2,§] and H. Franklin Bunn[2,3,*]

Department of Medicine,[*] Hematology Division, Brigham and Women's Hospital, Department of Cell Biology,[†] Harvard Medical School, Boston, MA; and School of Allied Health,[§] University of Kansas Medical Center, Kansas City, KS

Abstract **NCB5OR is a novel flavoheme reductase with a cytochrome b5-like domain at the N-terminus and a cytochrome b5 reductase-like domain at the C terminus. *Ncb5or* knock-out mice develop insulin deficient diabetes and loss of white adipose tissue. *Ncb5or*$^{-/-}$ mice have impairment of Δ9 fatty acid desaturation with elevated ratios of palmitate to palmitoleate and stearate to oleate. In this study we assess the role of the endoplasmic reticulum (ER) stress response in mediating lipotoxicity in *Ncb5or*$^{-/-}$ mice. The ER stress response was assessed by induction of BiP, ATF3, ATF6, XBP-1, and C/EBP homologous protein (CHOP). Exposure to palmitate, but not oleate or mixtures of oleate and palmitate induced these markers of ER stress to a much greater extent in *Ncb5or*$^{-/-}$ hepatocytes than in wild-type cells. In contrast, *Ncb5or*$^{-/-}$ and *Ncb5or*$^{+/+}$ hepatocytes were equally sensitive to ER stress imposed by increasing concentrations of tunicamycin. In order to assess the role of ER stress in vivo, we prepared mice that lack both NCB5OR and CHOP, a proapoptotic transcription factor important in the ER stress response. Onset of hyperglycemia in the *Chop*$^{-/-}$;*Ncb5or*$^{-/-}$ mice was delayed two weeks beyond that observed in *Chop*$^{+/+}$;*Ncb5or*$^{-/-}$ mice. Taken together these results suggest that ER stress plays a critical role in palmitate-induced lipotoxicity both in vitro and in vivo.**—Zhang, Y., K. Larade, Z-g. Jiang, S. Ito, W. F. Wang, H. Zhu, and H. F. Bunn. **The flavoheme reductase Ncb5or protects cells against endoplasmic reticulum stress-induced lipotoxicity. *J. Lipid Res.* 2010.** 51: **53–62.**

Supplementary key words reductase • endoplasmic reticulum • hyperglycemia • lipotoxicity • diabetes • lipoatrophy

Genome scans have uncovered multiple loci that are linked to both type 1 (1, 2) and type 2 (3) diabetes. In addition a number of other gene products play essential roles in β-cell function and viability. NCB5OR, also known as b5+b5R and Cyb5r4, is a novel, highly conserved NAD(P)H flavoheme reductase that contains a cytochrome b5-like domain at the N-terminus and a cytochrome b5 reductase-like domain at the C terminus (4, 5). It is localized in the endoplasmic reticulum (ER) and is ubiquitously expressed, with relatively high mRNA levels in the pancreas, heart, and kidney. *Ncb5or*$^{-/-}$ mice are glucose intolerant at ~4 weeks of age and at ~6 weeks of age develop frank diabetes (6). Serum insulin levels decrease with age, mirroring the reduced insulin content and progressive loss of β-cells in pancreatic islets. In addition, following birth, *Ncb5or*$^{-/-}$ mice develop lipoatrophy with progressive loss of white adipose tissue. This metabolic defect is observed even when diabetes has been prevented by early insulin treatment and pancreatic islet transplantation (7).

In keeping with the above-mentioned homology with classical cytochrome b5 and cytochrome b5 reductase, we investigated whether NCB5OR might provide an alternative source of electrons for fatty acid desaturation and recently reported that, indeed, *Ncb5or*$^{-/-}$ mice have a defect in the Δ-9 pathway (7). We found that the triglycerides, diacylglycerides, free fatty acids, and cholesterol esters in the liver of knock-out mice have 50–80% reduction in the ratios of palmitoleate to palmitate and oleate to stearate. This finding led to the hypothesis that diabetes in *Ncb5or*$^{-/-}$ mice is due at least in part to toxic effects of saturated fatty

This work was supported by grants from the Juvenile Diabetes Research Foundation to K.L. (3-2005-232) and H.F.B. (1-2005-121), the American Diabetes Association (7-04-RA-15) to H.F.B., and an RO1 grant from the National Institutes of Health (DK067355-A2) to H.F.B. and H.Z. Its contents are solely the responsibility of the authors and do not necessarily represent the official views of the National Institutes of Health.

Manuscript received 30 March 2009 and in revised form 29 June 2009.

Published, JLR Papers in Press, July 16, 2009
DOI 10.1194/jlr.M900146-JLR200

Abbreviations: ATF, activated transcription factor; BiP, glucose related protein 78 or GRP78; CHOP, C/EBP homologous protein; ER, endoplasmic reticulum; GTT, glucose tolerance test; H-E, hematoxylin and eosin; IRE, inositol requiring enzyme; KO, knock-out; PERK, double stranded RNA-activated protein kinase-like ER kinase; ROS, reactive oxygen species; SCD, stearoyl CoA desaturase; WT, wild-type; XBP-1, X-box binding protein 1.

[1] These authors made equal contributions to this work.
[2] These authors also made equal contributions to this work.
[3] To whom correspondence should be addressed.
e-mail: hfbunn@rics.bwh.harvard.edu
[S] The online version of this article (available at http://www.jlr.org) contains supplementary data in the form of one table and two figures.

acids. Although it was not technically feasible to carry out in vitro experiments on isolated pancreatic β-cells, we did show that the viability of isolated *Ncb5or*$^{-/-}$ hepatocytes was markedly impaired and apoptosis enhanced by incubation with palmitate but not with oleate or a mixture of palmitate and oleate (7).

There is growing evidence that in a number of cell types (8, 9), including pancreatic β-cells (10), the ER is a target of lipotoxicity induced by palmitate. Saturated fatty acids have been shown to induce stress in the ER, triggering a set of intracellular events initially designated the unfolded protein response (11–13). Pancreatic β-cells are particularly prone to ER stress (14–17).

An ER chaperone protein, BiP (also known as GRP78) serves as sensor and master regulator of the ER stress response. In the unstressed cell, BiP binds to three effector transmembrane ER proteins, the kinase and endoRNase IRE-1, the basic leucine-zipper activated transcription factor 6 (ATF-6), and the double stranded RNA-activated protein kinase-like ER kinase (PERK). When unfolded protein accumulates in the ER, it binds competitively to BiP, thereby freeing up IRE-1, PERK, and ATF-6 so that they homodimerize and are activated by transphosphorylation. Activated IRE-1 has RNase activity that cleaves an mRNA precursor of X-box binding protein (XBP)-1, enabling a frameshift that encodes mature XBP-1. This transcription factor regulates a subset of ER-resident chaperone genes that are essential for protein folding, maturation, and degradation in the ER, including CHOP (C/EBP homologous protein) (18). ATF-6 regulates a group of genes encoding ER-resident molecular chaperones and genes encoding folding enzymes.

In this paper, we have investigated the contribution of the ER stress response to enhanced lipotoxicity in *Ncb5or*$^{-/-}$ hepatocytes by assaying expression of BiP, mature XBP-1, CHOP, ATF-6, and a related transcription factor ATF-3 (19), all of which are upregulated during ER stress. In addition, we have assessed the in vivo contribution of CHOP expression to the development of diabetes in *Ncb5or*$^{-/-}$ mice.

EXPERIMENTAL PROCEDURES

Antibodies and reagents

Anti-GRP78/BiP (GL-19) antibody was obtained from Sigma (St Louis, MO); anti-SCD1 (S-15) and anti-cytochrome b5 (H-114), anti-XBP-1 (M-186), anti-CHOP (GADD153 B-3), and anti-ATF3 (H-90) antibodies from Santa Cruz Biotechnology (Santa Cruz, CA), and anti-β-actin antibody from Ambion, Inc. (Austin, TX). Palmitic acid, oleic acid, fatty acid free BSA and tunicamycin were purchased from Sigma. FFA stock solutions were prepared in 5% FFA-free BSA as previously described (7) and stored in liquid nitrogen to prevent oxidation. The final concentration of fatty acid was measured using a NEFA-HR [2] kit (Wako Chemicals, Richmond, VA), and adjusted to 5 mM.

RNA isolation, RT-PCR, and real-time quantitative PCR

Total RNA was extracted using Trizol reagent (Invitrogen, Carlsbad, CA) according to the manufacturer's instructions. In each reaction, 1μg total mRNA was used as template to perform RT-PCR using the Access RT-PCR system (Promega, Madison, WI). Primers used for RT-PCR include: *XBP-1* forward: 5′-TTA CGG GAG AAA ACT CAC GGC-3′, *XBP-1* reverse: 5′-GGG TCC AAC TTG TCC AGA ATG C-3′(20), *Chop* forward: 5′- GAA AGC AGA ACC TGG TCC ACG T-3′, *Chop* reverse: 5′-ATG TGC GTG TGA CCT CTG TTG- 3′ (21). For analysis of *Xbp-1* splicing, a 289 bp amplicon was generated from unspliced *Xbp-1*; a 263 bp amplicon was generated from spliced *Xbp-1*. PCR products were separated on a 2.5% agarose gel and stained with ethidium bromide.

For quality control, the RNA samples were analyzed by 1.5% agarose electrophoresis. The cDNA was synthesized using a High Capacity RNA-to-cDNA kit (Applied Biosystems, Foster City, CA). Each PCR reaction (1μg total RNA) was performed using optical 96-well reaction plates (Applied Biosystems) and the ABI Prism 7300 sequence detection machine employing SYBR Green PCR Master Mix (Applied Biosystems). The primer sequences used were as follows: *GAPDH* forward: 5′-TGT GTC CGT CGT GGA TCT GA-3′; *GAPDH* reverse: 5′-CCT GCT TCA CCA CCT TCT TGA-3′; *GADD153(Chop)* forward: 5′-ATG AAG GAG AAG GAG CAG GAG AA-3′; *GADD153(Chop)* reverse: 5′-CTT GGT GCA GGC TGA CCA TG-3′; *ATF3* forward: 5′-CGC CAT CCA GAA TAA ACA CC-3′; *ATF3* reverse: 5′-GCAGGCACTCTGTC-TTCTCC-3′; *ATF6* forward: 5′-GGA TTT GAT GCC TTG GGA GTC AGA C-3′; *ATF6* reverse: 5′-ATT TTT TTC TTT GGA GTC AGT CCA T-3′. All measurements were carried out in 20 μl volumes in triplicate, using mouse *GAPDH* mRNA levels for normalization. Average Ct values were recorded in triplicate and mRNA-level differences were calculated assuming that every cycle doubled the fluorescent intensity. To verify specificity, the products were analyzed by their melting curves and gel electrophoresis.

Western blotting

Cells were collected at specified time points during the incubations. After washing with PBS, cells were lysed in RIPA lysis buffer (Santa Cruz Biotechnology). Lysates were cleared by centrifugation and after determining protein concentration of the supernatants, 30 μg samples were prepared and separated on SDS-PAGE, transferred to polyvinylidene fluoride membrane (Millipore), and immunoblotted with the indicated primary antibody. β-actin protein expression was used as an internal loading standard. Signals were detected by ECL Plus Western Blot Detection System (Piscataway, NJ) and exposed on Fuji Medical X-ray film (Fujifilm Corporation, Tokyo, Japan).

Mouse hepatocyte isolation and cell culture

Mouse hepatocytes were prepared from 3- to 4-week-old wild-type and *Ncb5or*$^{-/-}$ male and female animals by the two-step perfusion procedure using Liver Perfusion Medium (Invitrogen) and Liver Digestion Medium (Invitrogen) separately as described previously (7). After isolation, hepatocytes were cultured in Williams' medium E (Invitrogen) containing penicillin/streptomycin and glutamine for 12 h before any treatment. The method we are currently using for hepatocyte isolation is considerably improved over that which we had previously employed and reported (7), both in yield and cell viability. We are now able to culture wild-type hepatocytes over a 24 h incubation period with <20% cell loss. After preincubation, cells were treated in Williams' medium E containing: fatty acid free BSA only (control) or with different concentrations of palmitate or oleate as indicated. Adequate fatty acid free BSA was supplemented into the medium and adjusted to a final concentration of 0.5%. Wild-type cells treated for 12 h with tunicamycin (1μg/ml) were used

as a positive control. In the tunicamycin sensitivity experiment, after preincubation, isolated cells were treated for 12 h with vehicle (DMSO) control or different concentrations of tunicamycin (0.2, 1, and 5 μg/ml).

Annexin V binding and TUNEL assay

Isolated hepatocytes were analyzed following incubation with fatty acid to detect apoptosis by using PE-Annexin V staining (ApoAlert Annexin V Apoptosis Kit, Clontech, Palo Alto, CA), and an in situ cell death detection kit (Fluorescein, Roche Applied Science). Cells were washed with cold PBS and incubated with PE-Annexin V. PE-Annexin V stained positive cells were determined by fluorescence microscopy (Nikon Eclipse TE300 microscope) using a rhodamine filter. TUNEL positive cells were identified and counted as described previously (7).

Transmission electron microscopy

The isolated hepatocytes were cultured in 6-well culture dishes and treated accordingly. At appropriate times, the liver cells that were attached to the bottom of the wells were fixed with 2.5% glutaraldehyde, 2% paraformaldehyde, and 0.02% picric acid in 0.1 M cacodylate buffer. While still in the wells, the cells were post fixed with 1% osmium tetroxide and 1.5% potassium ferrocyanide for one h. After washing in water and 0.5% maleate buffer (pH 5.2), the cells were treated with 1% uranyl acetate in maleate buffer and washed with water. The cells in the wells were dehydrated with graded cold ethanol, warmed to room temperature, and while in the last absolute ethanol dehydration step, each well was scored with a fine dissecting needle into tiny squares of 1 to 2 mm. In the next step, when propylene oxide was added, the solution was repeatedly flushed with the pipette until the cells were detached from the culture dish and transferred to a centrifuge tube and centrifuged into a pellet. The pellet was then treated like a piece of tissue and embedded in Epon Araldite. Thin sections were placed on bare grids and stained with saturated uranyl acetate in equal parts of acetone. Following lead citrate and staining, sections were examined and images were digitally recorded with a JEOL 1200 EX electron microscope.

Generation and identification of *Ncb5or*$^{-/-}$ mice in *Chop*$^{-/-}$ background

All procedures involving animals were approved by the Animal Care and Use Committee of Brigham and Women's Hospital and Children's Hospital in Boston. Mice were housed in a pathogen-free barrier facility on a 12 h light/12 h dark cycle on a standard rodent chow (Prolab Isopro RMH 3000 5P76). *Ncb5or*$^{-/-}$ mice, in which exon 4 was replaced with a *Pgk-Hyg* expression cassette, have been described previously (6). *Ncb5or*-deficient mice used in the present study were established on a virtually pure C57BL/6 (B6) background (>12 generations).

Chop$^{+/-}$ mice on a B6 background (22) were obtained from the Jackson Laboratory (Bar Harbor, ME). *Ncb5or*$^{+/-}$ heterozygotes bred into a pure B6 background were crossed with homozygous *Chop* KO mice (*Chop*$^{-/-}$), generating *Chop*$^{+/-}$;*Ncb5or*$^{+/-}$ and *Chop*$^{+/-}$;*Ncb5or*$^{+/+}$ mice. *Chop*$^{+/-}$;*Ncb5or*$^{+/-}$ mice were crossed with *Chop*$^{+/-}$;*Ncb5or*$^{+/-}$ or *Chop*$^{-/-}$;*Ncb5or*$^{+/-}$ mice, producing each of the genotypes in this study, including *Chop*$^{+/+}$;*Ncb5or*$^{+/+}$, *Chop*$^{+/+}$;*Ncb5or*$^{-/-}$, *Chop*$^{-/-}$;*Ncb5or*$^{+/+}$, and *Chop*$^{-/-}$;*Ncb5or*$^{-/-}$. Mice were genotyped by PCR using the following primers: *i*) *Ncb5or*: 5′-GTG AAC ACT AAT GCA TAC TCC CAG TCT GTG ATG C-3′; 5′-TGG AAC AGC AGG CTT CAC AGC- 3′; and 5′-GCG CCT ACC GGT GGA TGT GGA A-3′; *ii*) *Chop* forward: 5′- GCA GCC ATG GCA GCT GAG TCC CTG CCT TCC-3′; *Chop* reverse: 5′- CAG ACT CGA GGT GAT GCC CAC TGT TCA TGC– 3′. The thermal cycle reaction was performed as follows: 94°C for 2 min, followed by 35 cycles at 94°C for 15 s, 55°C for 30 s, 68°C for 2 min, and an additional step of 72°C for 7 min at the end.

Blood glucose measurements

Blood glucose concentration was measured using the One Touch blood glucose monitoring system (Lifescan). Intraperitoneal glucose tolerance tests (GTT) were performed after a 10 to 12 h fast (2 mg dextrose/g body weight). Blood samples for GTT were obtained from tail veins at 0, 15, 30, 60, and 120 min after injection.

Immunostaining

Tissue for analysis was fixed in either buffered 4% paraformaldehyde solution or Bouin's solution, embedded in paraffin, and sectioned for analysis. Slides were stained with hematoxylin and eosin (H-E) for islet identification and analysis. Insulin was detected by guinea pig anti-human insulin (Linco) diluted 1:100, followed by incubation with peroxidase-conjugated AffiniPure goat anti-rabbit Ig (H+L) (Jackson ImmunoResearch) diluted 1:1000. A 3,3-diaminobenzidine tetrahydrochloride (DAB) staining kit (Vector) was used as the substrate for peroxidase. Sections were counterstained by hematoxylin.

Statistics

All of the error bars shown in the figures are mean ± standard deviation. Statistical significance was calculated by the Student's *t*-test.

RESULTS

Palmitate impairs cell viability and induces apoptosis in *Ncb5or*$^{-/-}$ hepatocytes

We previously reported that primary hepatocytes from *Ncb5or*$^{-/-}$ (KO) mice had impaired viability and enhanced apoptosis, analyzed by TUNEL, following 1 h and 4 h exposure to 1.0 mM palmitate but not to 1.0 mM oleate or an equimolar mixture of the two fatty acids (7). With a greatly improved method for cell isolation, we are now able to obtain cells at much higher yields and improved viability, allowing longer incubation times. Supplementary Fig. I shows responses to lower, more physiologic levels of palmitate: 0.1, 0.25, and 0.5 mM, following a 12 h incubation. Increased cell death, as assessed by trypan blue exclusion, and enhanced apoptosis, as determined by Annexin V staining and TUNEL, were induced in KO but not in wild-type (WT) cells by a 12 h exposure to as little as 0.1 mM palmitate. Primary hepatocytes are inherently heterogeneous. Even with an improved isolation method, 25% of WT and KO cells were nonviable in the absence of exposure to palmitate and following incubation with 0.5 mM palmitate, 65% of KO cells were nonviable. The experiments reported below pertain to cells that remained viable after 12 h and 24 h incubations.

Palmitate but not oleate induces markers of ER stress in KO hepatocytes

The ER stress response in cells generally includes induction of a number of transcripts including spliced XBP-1 and the CHOP transcription factor. Tunicamycin, an agent that causes a marked impairment in N-linked glycosylation

of proteins, is commonly used as a positive control to trigger the ER stress response. As shown in **Fig. 1A**, tunicamycin induced both the spliced XBP-1 transcript and *Chop* mRNA in WT hepatocytes. Treatment with 0.5 mM palmitate induced both the spliced XBP-1 (Fig. 1A) and *Chop* mRNA (Fig. 1A and B) in KO cells but not in WT cells. In contrast, treatment with 0.5 mM oleate failed to induce either the spliced XBP-1 or *Chop* transcripts, a result consistent with the impairment of cell viability and enhancement of apoptosis imposed by saturated palmitate [supplementary Fig. I and Larade et al. (7)] but not by monounsaturated oleate (7). In like manner, as shown in Figs. 1C and D, palmitate induced mRNA expression of two other markers of ER stress, ATF3 and ATF6, in KO cells but not in WT cells. In contrast, no significant induction was noted in either WT type or KO cells following exposure to oleate.

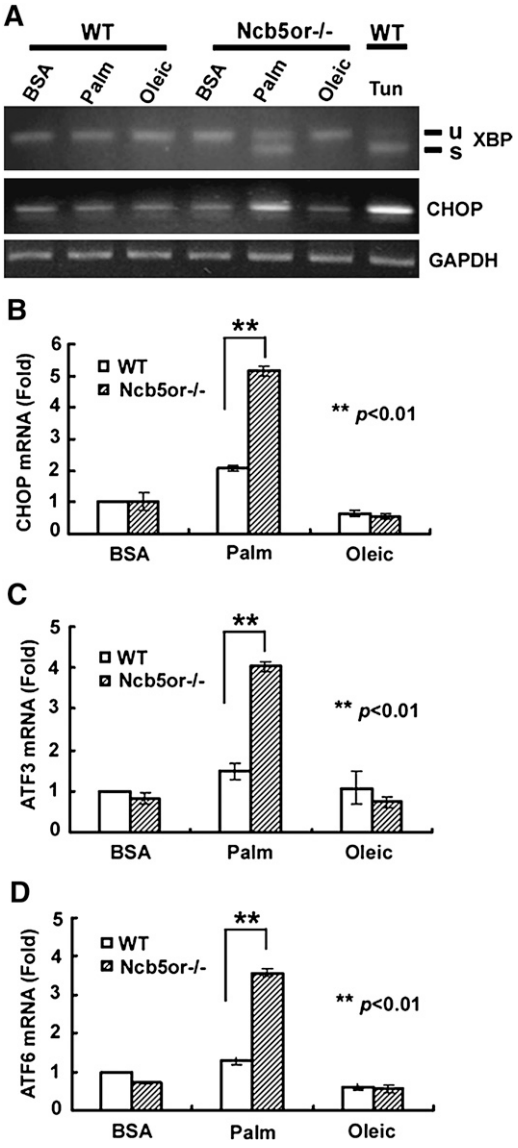

Fig. 1. mRNA markers of ER stress. Primary hepatocytes were incubated for 12 h with fatty acid depleted BSA, 0.5 mM palmitate or 0.5 mM oleate. A: *Xbp-1* mRNA splicing and *Chop* mRNA expression was determined by RT-PCR. Unspliced (u) and spliced (s) *Xbp-1* products are indicated. Tunicamycin treated wild-type cells (Tun) served as a positive control for ER stress. Glyceraldehyde-3-phosphate dehydrogenase (GAPDH) transcript levels served as internal control for RNA loading. B, C and D: Normalized *Chop*, *ATF3*, and *ATF6* mRNA levels were measured in samples by quantitative PCR and are shown relative to levels in wild-type cells treated only with BSA. Asterisks represent statistically significant differences between KO and WT: ** $P < 0.01$. (n = 3 animals/genotype). Error bars indicate mean ± SD.

We also examined markers of ER stress at the protein level. As shown in **Fig. 2A**, following incubation with 0.5 mM palmitate, BiP, the master regulator of the ER stress response (see above), was induced in KO cells but not in WT cells. As expected, treatment of wild-type hepatocytes with tunicamycin (1 μg/ml for 12 h) also induced BiP along with the other markers of ER stress shown in this figure. The level of BiP protein was further enhanced in KO cells by a longer (24 h) incubation (not shown). Palmitate incubation also induced expression of the 50 kDa N-terminal cleavage product of ATF6 (23), as well as CHOP and ATF3. In like manner, as shown in Fig. 2B, palmitate induced XBP-1 protein in KO but not in WT hepatocytes. Stearoyl CoA desaturase-1 (SCD-1) and microsomal cytochrome b5 (Cyt b5) protein expression were induced somewhat by palmitate in both KO and WT cells whereas expression in WT cells was not affected by tunicamycin.

KO and WT hepatocytes were incubated for 12 h with 0, 0.1, 0.25, and 0.5 mM palmitate. No significant induction of the spliced *XBP-1* mRNA, nor of *Chop*, *ATF3*, or *ATF6* mRNAs were noted with 0.1 mM palmitate whereas exposure to 0.25 and 0.5 mM palmitate resulted in robust induction of all four markers of ER stress (**Fig. 3**). This dose response closely mimics the effect of increasing levels of palmitate on cell viability and apoptosis shown in Supplementary Fig. I.

Transmission electron microscopy

We examined ultrastructure of hepatocytes from three WT and three KO mice. Cells were incubated for 4, 12, and 24 h with 0.5 mM palmitate in 0.5% albumin versus the same concentration of lipid-depleted albumin. The integrity of the majority of the cells remained fully intact in all samples. Not surprisingly, WT and KO cells incubated in palmitate contained increased numbers of lipid droplets, many of which appeared crystalline. In all samples mitochondrial morphology and number were normal. No abnormalities were seen in cells incubated for 4 h and 12 h. Following 24-h incubation in palmitate, a substantial fraction of KO cells had only small amounts of rough ER with distension of the cisternae and decreased numbers of polyribosomes (**Fig. 4B**). In these cells, there were increased amounts of agranular or smooth surfaced ER, which were tubular in form. These changes were considerably less prominent in both KO cells treated with 0.5% albumin (Fig. 4A) and in WT cells treated with palmitate (Fig. 4C).

Reversal by oleate of ER stress induced by palmitate

A 12 h exposure of KO hepatocytes to 0.5 mM palmitate induced *Chop* mRNA as shown in Figs. 1A, 1B, and **5A**, lane

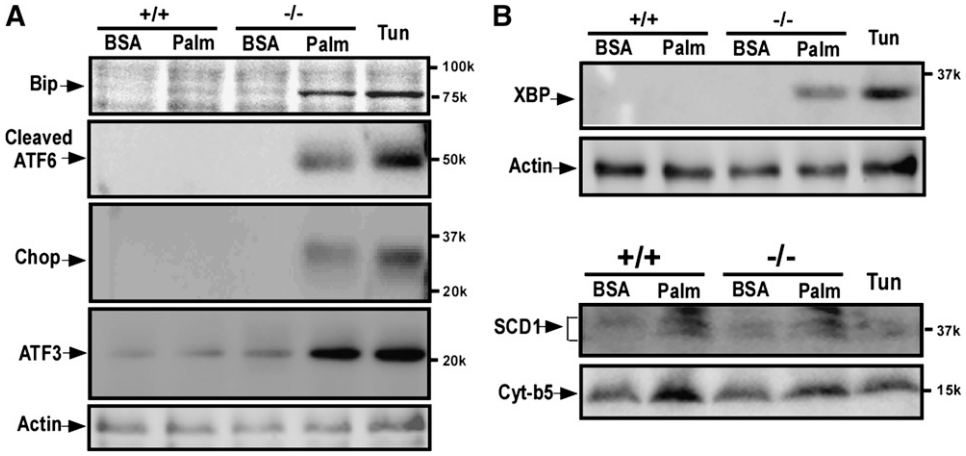

Fig. 2. Protein markers of ER stress. WT (*Ncb5or*$^{+/+}$) or KO (*Ncb5or*$^{-/-}$) primary hepatocytes were treated for 12 h with palmitic acid (0.5 mM) or fatty acid free BSA only. In addition WT hepatocytes were treated for 12 h with tunicamycin 1 μg/ml. A: BiP, the cleaved N-terminal fragment of ATF6, CHOP, and ATF3 were analyzed by Western blots. B: Top: Western blot determinations of XBP-1. Bottom: Western blot determinations of SCD1 and cytochrome b5. To normalize for protein loading, the same blots were reused for antibody detection of β-actin.

2. However, addition of increasing concentrations of oleate to the palmitate solution resulted in a reduction in *Chop* mRNA expression (Fig. 5A). At equimolar concentrations of palmitate and oleate (0.5 mM each), the expression of *Chop* mRNA was indistinguishable from that seen in cells not exposed to added fatty acids. In like manner, as shown in Fig. 5B, coincubation with increasing amounts of oleate gradually lowered the induction of CHOP and XBP-1 protein. ER stress imposed by palmitate can be reversed by subsequent exposure to oleate. KO hepatocytes were first incubated for 24 h in 0.5 mM palmitate and then incubated for an additional 12 h in either 0, 0.1, 0.25, or 0.5 mM oleate. As shown in Fig. 5C, the induction of *ATF6* mRNA was gradually abolished by the addition of increasing concentrations of oleate.

Sensitivity to tunicamycin

As mentioned above, inhibition of N-linked glycosylation by the agent tunicamycin impairs proper folding and trafficking of glycoproteins and is frequently used to assess cytologic and biochemical markers of the ER stress response. We exposed isolated hepatocytes to 12 h incubations in increasing concentrations of tunicamycin (0, 0.2, 1.0, and 5.0 μg/ml) and, as shown in **Fig. 6**, observed dose-dependent increases in expression of *Chop, ATF3 and ATF6* mRNAs and no difference between KO and WT cells in their sensitivity to tunicamycin.

Induction of *Ncb5or* mRNA in *Ncb5or*$^{+/+}$ hepatocytes by fatty acids

As shown in Supplementary Fig. IIA, following 12-h incubation of WT hepatocytes with increasing concentrations of palmitate (0.1, 0.25 and 0.5 mM), *Ncb5or* mRNA expression was enhanced up to about 3.3-fold that observed following incubation with albumin alone. Exposure to the same concentrations of oleate resulted in a more modest 2.5-fold induction. Incubation with an equimolar mixture (0.25 mM palmitate and 0.25 mM oleate) resulted in the same level of induction as 0.25 mM palmitate or 0.25 mM oleate alone. In contrast, tunicamycin (1μg/ml) had no effect on the expression of Ncb5or mRNA (Supplementary Fig. IIB).

Chop disruption delays onset of hyperglycemia

As shown above (Figs. 1, 2, 5), palmitate induces a robust increase in Chop mRNA and protein expression in KO hepatocytes. As mentioned above, ER stress is often preceded by upregulation of the *Chop* gene. CHOP is a known mediator of apoptosis via downregulation of Bcl-2 (24) and/or activation of caspase 3 (13). We hypothesized that absence of CHOP expression might enhance β-cell survival in *Ncb5or*$^{-/-}$ mice and delay the onset of diabetes. *Chop*$^{-/-}$ mice are fertile and produce viable fully developed offspring, which have normal glucose tolerance and insulin sensitivity (25). B6*Ncb5or*$^{+/-}$ mice were bred with B6 *Chop*$^{-/-}$ mice producing four genotypes: *Ncb5or*$^{+/+}$,*Chop*$^{+/+}$; *Ncb5or*$^{+/+}$,*Chop*$^{-/-}$; *Ncb5or*$^{-/-}$,*Chop*$^{+/+}$ and *Ncb5or*$^{-/-}$,*Chop*$^{-/-}$. These genotypes were identified by PCR as shown in **Fig. 7A**.

These mice were used to assess whether absence of CHOP expression had any impact on the two main phenotypes seen in *Ncb5or*$^{-/-}$ mice, lipoatrophy and diabetes. As shown in Fig. 7B, after ~6 weeks of age, wild-type B6 mice (*Ncb5or*$^{+/+}$,*Chop*$^{+/+}$) continue to gain weight owing to progressive accumulation of white adipose tissue. In contrast, the weights of B6*Ncb5or*$^{-/-}$; *Chop*$^{+/+}$ mice plateau after ~6 weeks because normal somatic growth is offset by of a progressive loss of white adipose tissue content. We had previously made the same observation in *Ncb5or*$^{-/-}$ bred into a pure Balb/c genetic background (6, 7). As shown in Fig. 7B, absence of CHOP expression had no significant impact on the weight profiles of either *Ncb5or*$^{+/+}$ or *Ncb5or*$^{-/-}$ mice.

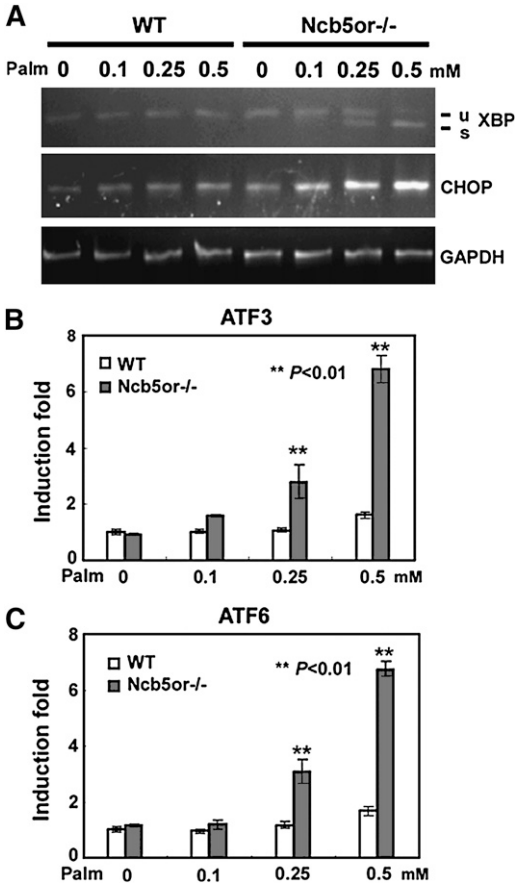

Fig. 3. Dose response to palmitic acid (Palm) in wild-type and Ncb5or/- cells. A: WT and KO primary hepatocytes were treated with 0, 0.1, 0.25, and 0.5 mM palmitic acid for 12 h. Total RNA was extracted from cells and subjected to RT-PCR for analysis of *XBP-1* splicing, *Chop* and *GAPDH* mRNA expression. B: *ATF3* and C. *ATF6* mRNA expression were determined by quantitative PCR. Asterisks represent statistically significant differences between KO and WT: ** $P < 0.01$. (n = 3 animals/genotype). Error bars indicate mean ± SD.

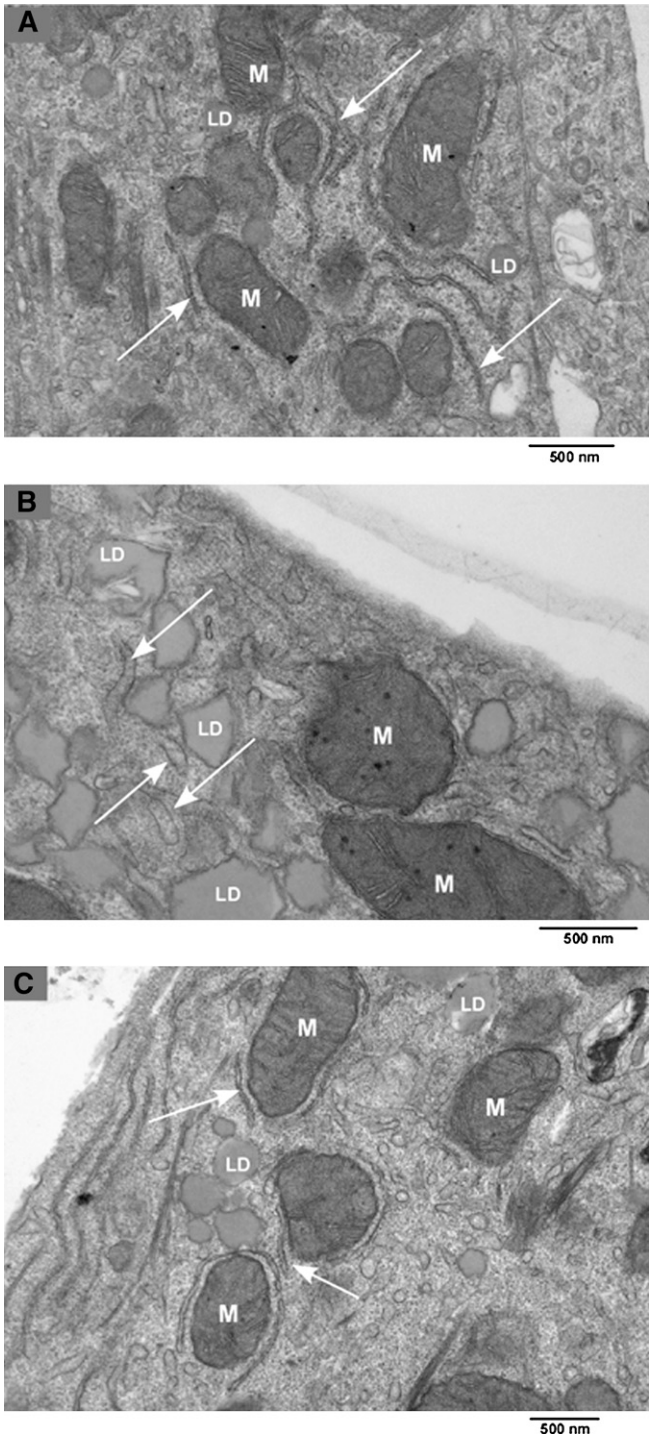

Fig. 4. Effect of palmitic acid treatment on ultrastructure of KO and WT hepatocytes. Following 24 h incubations of KO and WT hepatocytes with either 0.5 mM palmitate or fatty acid free BSA, specimens were prepared for transmission electron microscopy. A: KO, BSA. B: KO, palmitate. C: WT, palmitate. M, mitochondrion; LD, lipid droplet. Arrow points to rough endoplasmic reticulum.

In like manner, as shown in Fig. 7C, the presence or absence of CHOP expression had no detectable effect on the H-E morphology of islets from either B6*Ncb5or*$^{+/+}$ or B6*Ncb5or*$^{-/-}$ 5-week-old mice. Irrespective of whether or not the mice expressed CHOP, the islets of the *Ncb5or*$^{-/-}$ mice were smaller than those of *Ncb5or*$^{+/+}$ mice and contained less insulin.

We assessed whether loss of *Chop* impacts the onset and severity of diabetes in *Ncb5or*$^{-/-}$ mice. In 3.5-week-old animals, no difference in glucose tolerance was observed between any of the genotypes (**Fig. 8A**). At 4 and 5 weeks of age (Fig. 8B,C), *Ncb5or*$^{-/-}$ animals were glucose intolerant in both *Chop*$^{+/+}$ and *Chop*$^{-/-}$ backgrounds, although at the 120 min time point, all genotypes had returned to basal glucose levels. At 6 weeks of age (Fig. 8D), *Chop*$^{-/-}$;*Ncb5or*$^{-/-}$ animals remained glucose intolerant but glucose returned to basal levels at the 120 min time point, similar to the levels obtained by *Ncb5or*$^{+/+}$ animals. In contrast, blood glucose levels in *Chop*$^{+/+}$;*Ncb5or*$^{-/-}$ animals remained high at the 120 min time point, suggesting a greater deficit of functioning β-cells. Fasting blood glucose was measured in mice up to 10 weeks (Fig. 8E) with *Ncb5or*$^{+/+}$ remaining normoglycemic for the entire time course, regardless of *Chop* genotype. The *Chop*$^{+/+}$;*Ncb5or*$^{-/-}$ mice became hyperglycemic between 5.5 and 6 weeks as expected. Onset of hyperglycemia in the *Chop*$^{-/-}$;*Ncb5or*$^{-/-}$ mice was delayed until 7.5–8 weeks of age, a finding consistent with the GTT results. Taken together, the results presented here suggest

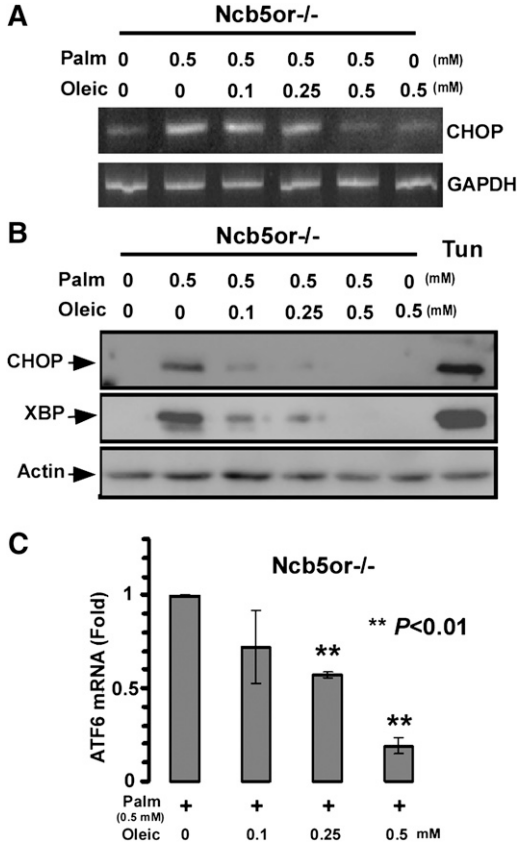

Fig. 5. Effect of oleic acid on palmitic acid induced ER stress. A, B: Hepatocytes were incubated with either 0 or 0.5 mM palmitate alone or 0.5 mM palmitate (Palm) mixed with increasing concentrations of oleic acid (0.1, 0.25 and 0.5 mM) for 12 h. A: *Chop* and *GAPDH* mRNA expression was determined by RT-PCR. B: Western blot determination of expression of CHOP and XBP-1 protein. C: After treatment of isolated hepatocytes with palmitate (0.5 mM) for 24 h, oleic acid was added at the indicated concentrations. After a further 12 h incubation, cells were collected for analysis of *ATF6* mRNA. (n = 3 animals/genotype) Asterisks represent significant differences between presence and absence of oleate. Error bars indicate mean ± SD.

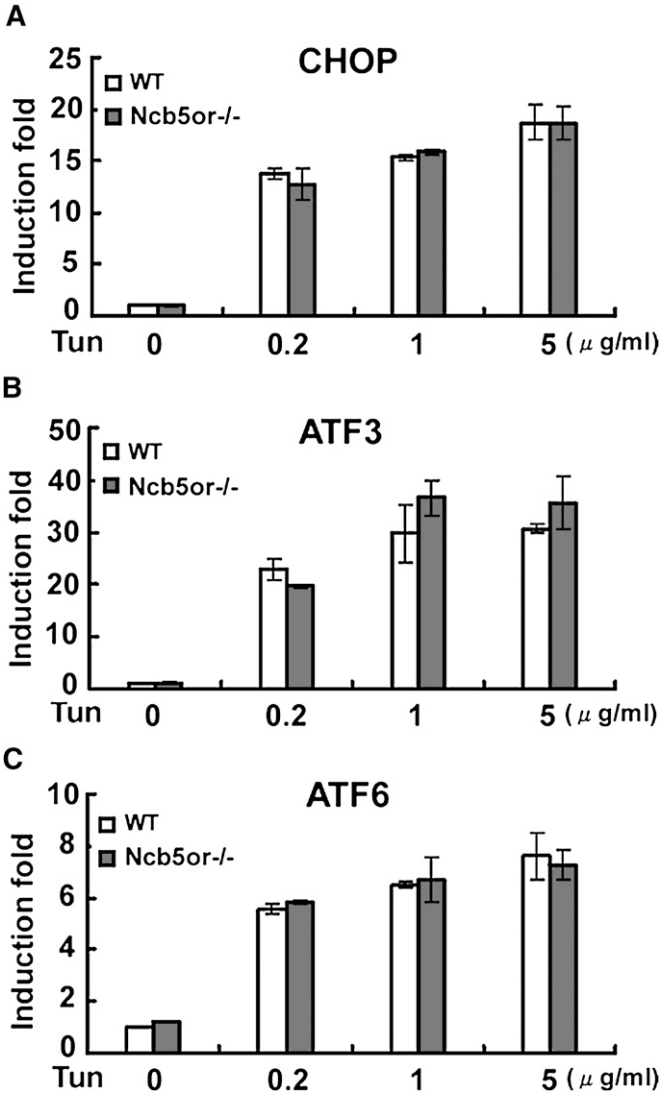

Fig. 6. Sensitivity to tunicamycin. Isolated primary hepatocytes from wild-type mice and NCB5OR null mice were treated for 12 h with increasing concentrations of tunicamycin. After cell collection, total RNA was extracted from each sample. *Chop*, *ATF3*, and *ATF6* mRNA were determined by quantitative PCR. No significant differences were noted between KO and WT cells at each dose of tunicamycin (n = 3 animals/genotype). Error bars indicate mean ± SD.

that CHOP-mediated apoptosis contributes significantly to β-cell loss in B6*Ncb5or*$^{-/-}$ mice.

DISCUSSION

Because the primary phenotype of *Ncb5or-/-* mice is diabetes and lipoatrophy, pancreatic β-cells and adipocytes would be the most relevant primary cell types to investigate ER stress. However, despite repeated attempts, we were not able to carry out experiments on these cells owing to their enhanced fragility and low preparative yields. Accordingly, we used primary hepatocytes. We were able to obtain good yields by collagenase perfusion of livers of 3- to 4-week-old WT and KO mice. At this age, the animals are normoglycemic and have normal deposits of white adipose tissue. Therefore, the hepatocytes obtained from KO mice are unlikely to be affected by metabolic perturbations in older KO animals.

Our experiments on primary hepatocytes show that cells from mice deficient in NCB5OR do not display any markers of ER stress when examined under standard incubation conditions. However, upon exposure to increasing concentrations of the saturated fatty acid palmitate, five independent markers of ER stress become positive. In contrast, ER stress was not seen following treatment with monounsaturated oleate or in mixtures of palmitate and oleate and could be reversed by the subsequent addition of oleate to palmitate treated cells (Fig. 5). These results must be interpreted in the light of previous studies in which we found no differences in five different organs of wild-type versus either prediabetic or diabetic KO mice in the expression of *Bip*, *Chop*, or mature *XBP-1* mRNA (26). Moreover, nearly complete knockdown of *Ncb5or* mRNA

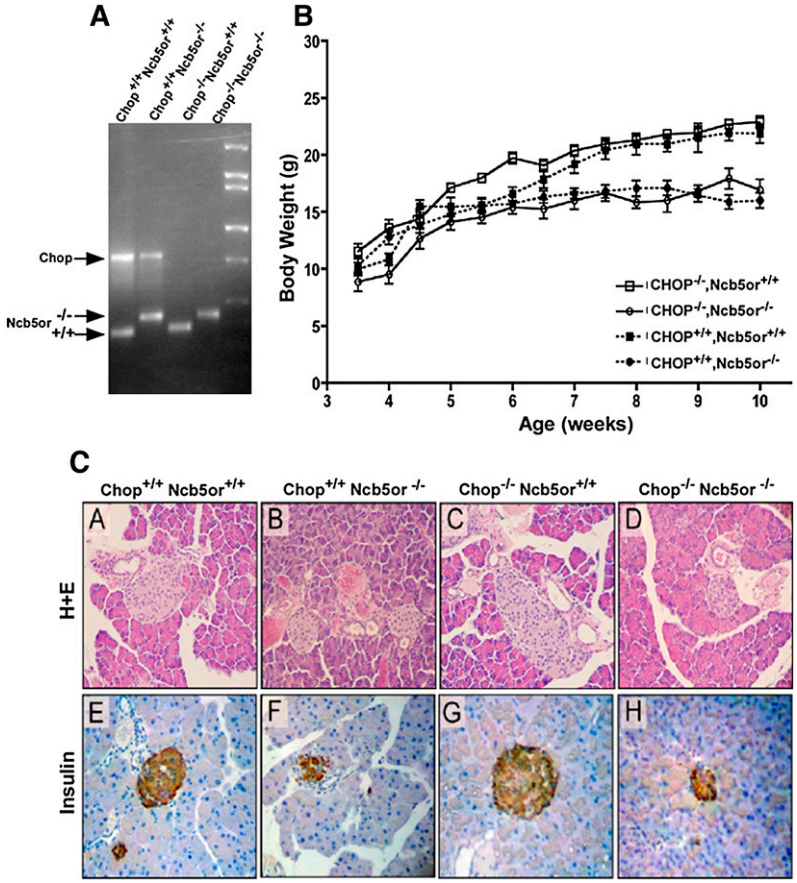

Fig. 7. Characterization of *Ncb5or/Chop*-null mice. A: Genotyping of experimental animals by PCR. B: Body weight was measured and recorded biweekly for each genotype, starting shortly after weaning at 3.5 weeks and monitored up to 10 weeks of age (n = 8 animals per genotype). In mice older than 7.5 weeks, Ncb5or$^{-/-}$ mice weighed significantly less than Ncb5or$^{+/+}$ mice, irrespective of CHOP genotype ($P < 0.001$). C: Pancreatic slides prepared on 5-week-old mice from each genotype were stained with i) hematoxylin and eosin (A–D), ii) insulin (E–H). Representative samples are shown for each genotype. (× 300 magnification).

expression in βTC3 insulinoma cells failed to induce either *Bip* or *Chop* mRNA. Finally, as shown in Fig. 6, KO hepatocytes did not differ from WT in their sensitivity to the ER stress-inducing agent tunicamycin.

Taken together, these observations suggest that ER stress in NCB5OR deficient cells is specific for the saturated fatty acid palmitate. The enhanced sensitivity of KO hepatocytes to palmitate is likely due to impairment in conversion of this saturated fatty acid to monounsaturated oleate. Our in vitro results as well as the in vivo results discussed below argue strongly that the principal biologic function of NCB5OR is in mediating fatty acid desaturation and protecting cells from lipotoxicity induced by saturated fatty acids.

Our results raise the question of how palmitate induces the ER stess response. In cardiomyocytes, exposure to palmitate results in mitochondrial swelling and release of cytochrome c, thus triggering apoptosis (27–29). However, neither our KO nor our WT cells revealed any abnormalities in mitochondrial ultrastructure even after 24 h incubation in palmitate. Palmitate may also impose a direct toxic effect on the ultrastructure of the endoplasmic reticulum. Borradaile et al. (9) found that exposure of Chinese hamster ovary (CHO) cells to 0.5 mM palmitate for 5 h resulted in marked dilatation of the rough ER, whereas, as shown in Fig. 5, we observed much less dramatic changes in the RER only after 24 h of incubation.

Reactive oxygen species (ROS) may be an important intermediate in ER stress induced by palmitate. In both cardiomyocytes (8) and CHO cells (30), palmitate-induced ER stress response was triggered at least in part by the generation of ROS. More recently, Song et al. (31) have shown that in the leptin receptor deficient model of diabetes, ROS are likely to mediate ER stress-dependent apoptosis of pancreatic β-cells in vivo. We have bred the Ncb5or null allele into mouse substrains selectively outbred for susceptibility (ALS) versus resistance (ALR) to the oxidant diabetogenic agent alloxan. In keeping with the likely contribution of ROS to ER stress-induced apoptosis of β-cells, we have found that glucose intolerance appeared earlier and was more pronounced in *Ncb5or*$^{-/-}$ mice in the ALS background versus those in the ALR background (K Larade, Z Jiang, C Matthews, H. Zhu and H. F. Bunn, unpublished observations).

In βTC3 insulinoma cells, a wide variety of metabolic and chemical perturbations (listed in supplementary Table I) failed to either induce or suppress endogenous *Ncb5or* mRNA expression (26, 32). Thus, we had concluded that *Ncb5or* is a "housekeeping" gene. However, as shown in supplementary Fig. II, *Ncb5or* mRNA expression in primary hepatocytes is induced by fatty acids, palmitate slightly more than oleate. This result also supports the notion that the prime biologic role of NCB5OR is in fatty acid metabolism.

The in vivo results presented in Figs. 7 and 8 also attest to the role of the ER stress response in the pathogenesis of diabetes in *Ncb5or*$^{-/-}$ mice. At 6 weeks of age, *Chop*$^{-/-}$;*Ncb5or*$^{-/-}$ mice maintained better glucose control

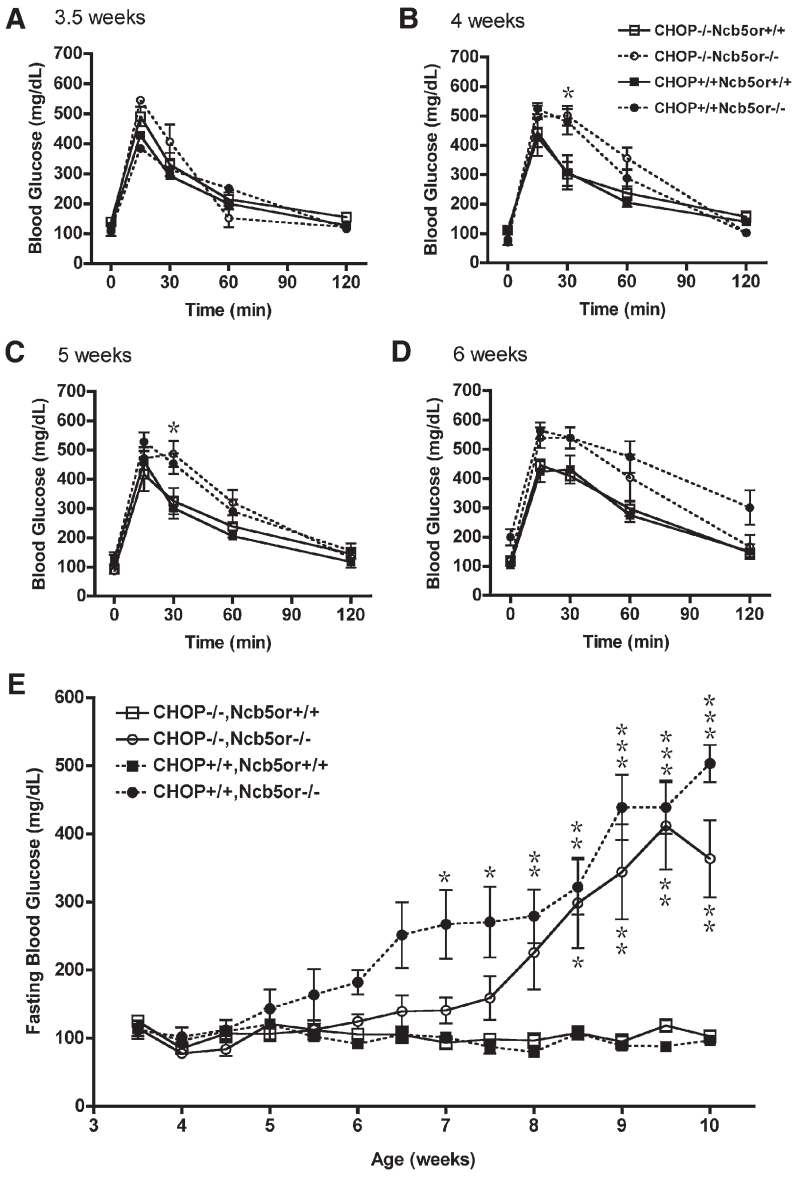

Fig. 8. Impact of NCB5OR and CHOP deficiency on glucose tolerance and onset of hyperglycemia. Glucose tolerance tests (GTTs) were performed bi-weekly on each genotype. Fasting blood glucose was measured prior to GTT and recorded following an overnight fast (12–14 h). GTTs (A–D) and fasting blood glucose measurements (E) were initiated on 3.5 week old pups shortly after weaning and were continued until mice were 6 weeks (A–D; n = 4 mice/genotype) and 10 weeks old (E; n = 8 mice/genotype), respectively. * $P < 0.05$, ** $P < 0.01$, *** $P < 0.001$.

relative to *Chop*$^{+/+}$;*Ncb5or*$^{-/-}$ mice, as demonstrated by GTT, as well as by a 2 week delay in onset of diabetes in the *Chop*$^{-/-}$;*Ncb5or*$^{-/-}$ mice. A similar result has been demonstrated with the Akita mouse, a monogenetic model of diabetes (33). A mutation of the insulin 2 gene (Ins2) disrupts a disulfide bond in insulin, inducing a conformational change leading to ER stress. These mice have reduced β-cell mass and become hyperglycemic but without insulitis or obesity. When Akita mice were bred into mice with a targeted disruption of the *Chop* gene, the onset of diabetes in Akita heterozygotes was delayed, a direct result of reduced β-cell apoptosis (34). Because the loss of expression of CHOP convincingly delays the onset of diabetes in the *Ncb5or*$^{-/-}$ mouse, it is likely that apoptosis mediated by ER stress is a major contributor to the reduction of β-cell viability imposed by *Ncb5or* deficiency.

Our in vivo results are very much in accord with a recent report by Song et al. (31) that assesses the impact of *Chop* depletion in three mouse models of diabetes: streptozotocin-induced β-cell damage, as well as mutations causing deficiency of leptin receptor, and impaired PERK-dependent phosphorylation of eIF2α. In all three models, loss of CHOP expression resulted in improved glucose tolerance similar to what we have observed in *Ncb5or*$^{-/-}$ mice.

Despite considerable effort, we have never been able to demonstrate enhanced apoptosis in β-cells of *Ncb5or*$^{-/-}$ mice. It is likely that the relatively slow attrition of β-cells over an ~4 week period precludes convincing documentation. Nevertheless, results in this report suggest that apoptosis triggered by ER stress contributes importantly to the demise of *Ncb5or*$^{-/-}$ β-cells. It is likely that the ER stress response in these cells is triggered at a very low threshold. Our in vivo experiment shown in Fig. 7 suggests that β-cell viability and function are retained for a significant period of time in *Chop*$^{-/-}$ mice when the ER stress response is bypassed. Thus, if humans are similar to mice, it is possible that pharmacologic inhibition of the ER stress response might prolong the viability of β-cells in patients with type 2 diabetes.

REFERENCES

1. Bartsocas, C. S., and A. Gerasimidi-Vazeou. 2006. Genetics of type 1 diabetes mellitus. *Pediatr. Endocrinol. Rev.* **3(Suppl 3):** 508–513.
2. Alizadeh, B. Z., and B. P. Koeleman. 2008. Genetic polymorphisms in susceptibility to Type 1 diabetes. *Clin. Chim. Acta.* **387:** 9–17.
3. Doria, A., M. E. Patti, and C. R. Kahn. 2008. The emerging genetic architecture of type 2 diabetes. *Cell Metab.* **8:** 186–200.
4. Zhu, H., H. Qiu, H. W. Yoon, S. Huang, and H. F. Bunn. 1999. Identification of a cytochrome b-type NAD(P)H oxidoreductase ubiquitously expressed in human cells. *Proc. Natl. Acad. Sci. USA.* **96:** 14742–14747.
5. Zhu, H., K. Larade, T. A. Jackson, J. Xie, A. Ladoux, H. Acker, U. Berchner-Pfannschmidt, J. Fandrey, A. R. Cross, G. S. Lukat-Rodgers, et al. 2004. NCB5OR is a novel soluble NAD(P)H reductase localized in the endoplasmic reticulum. *J. Biol. Chem.* **279:** 30316–30325.
6. Xie, J., H. Zhu, K. Larade, A. Ladoux, A. Seguritan, M. Chu, S. Ito, R. T. Bronson, E. H. Leiter, C. Y. Zhang, et al. 2004. Absence of a reductase, NCB5OR, causes insulin-deficient diabetes. *Proc. Natl. Acad. Sci. USA.* **101:** 10750–10755.
7. Larade, K., Z. Jiang, Y. Zhang, W. Wang, S. Bonner-Weir, H. Zhu, and H. F. Bunn. 2008. Loss of NCB5OR results in impaired fatty acid desaturation, lipoatrophy and diabetes. *J. Biol. Chem.* **283:** 29285–29291.
8. Borradaile, N. M., K. K. Buhman, L. L. Listenberger, C. J. Magee, E. T. Morimoto, D. S. Ory, and J. E. Schaffer. 2006. A critical role for eukaryotic elongation factor 1A–1 in lipotoxic cell death. *Mol. Biol. Cell.* **17:** 770–778.
9. Borradaile, N. M., X. Han, J. D. Harp, S. E. Gale, D. S. Ory, and J. E. Schaffer. 2006. Disruption of endoplasmic reticulum structure and integrity in lipotoxic cell death. *J. Lipid Res.* **47:** 2726–2737.
10. Diakogiannaki, E., H. J. Welters, and N. G. Morgan. 2008. Differential regulation of the endoplasmic reticulum stress response in pancreatic beta-cells exposed to long-chain saturated and monounsaturated fatty acids. *J. Endocrinol.* **197:** 553–563.
11. Kaufman, R. J. 1999. Stress signaling from the lumen of the endoplasmic reticulum: coordination of gene transcriptional and translational controls. *Genes Dev.* **13:** 1211–1233.
12. Mori, K. 2000. Tripartite management of unfolded proteins in the endoplasmic reticulum. *Cell.* **101:** 451–454.
13. Zhang, K., and R. J. Kaufman. 2004. Signaling the unfolded protein response from the endoplasmic reticulum. *J. Biol. Chem.* **279:** 25935–25938.
14. Harding, H. P., and D. Ron. 2002. Endoplasmic reticulum stress and the development of diabetes: a review. *Diabetes.* **51(Suppl 3):** S455–S461.
15. Araki, E., S. Oyadomari, and M. Mori. 2003. Endoplasmic reticulum stress and diabetes mellitus. *Intern. Med.* **42:** 7–14.
16. Laybutt, D. R., A. M. Preston, M. C. Akerfeldt, J. G. Kench, A. K. Busch, A. V. Biankin, and T. J. Biden. 2007. Endoplasmic reticulum stress contributes to beta cell apoptosis in type 2 diabetes. *Diabetologia.* **50:** 752–763.
17. Huang, C. J., C. Y. Lin, L. Haataja, T. Gurlo, A. E. Butler, R. A. Rizza, and P. C. Butler. 2007. High expression rates of human islet amyloid polypeptide induce endoplasmic reticulum stress mediated beta-cell apoptosis, a characteristic of humans with type 2 but not type 1 diabetes. *Diabetes.* **56:** 2016–2027.
18. Wang, X. Z., B. Lawson, J. W. Brewer, H. Zinszner, A. Sanjay, L. J. Mi, R. Boorstein, G. Kreibich, L. M. Hendershot, and D. Ron. 1996. Signals from the stressed endoplasmic reticulum induce C/EBP-homologous protein (CHOP/GADD153). *Mol. Cell. Biol.* **16:** 4273–4280.
19. Pan, Y., H. Chen, F. Siu, and M. S. Kilberg. 2003. Amino acid deprivation and endoplasmic reticulum stress induce expression of multiple activating transcription factor-3 mRNA species that, when overexpressed in HepG2 cells, modulate transcription by the human asparagine synthetase promoter. *J. Biol. Chem.* **278:** 38402–38412.
20. Lin, J. H., H. Li, D. Yasumura, H. R. Cohen, C. Zhang, B. Panning, K. M. Shokat, M. M. Lavail, and P. Walter. 2007. IRE1 signaling affects cell fate during the unfolded protein response. *Science.* **318:** 944–949.
21. Shirakawa, K., S. Maeda, T. Gotoh, M. Hayashi, K. Shinomiya, S. Ehata, R. Nishimura, M. Mori, K. Onozaki, H. Hayashi, et al. 2006. CCAAT/enhancer-binding protein homologous protein (CHOP) regulates osteoblast differentiation. *Mol. Cell. Biol.* **26:** 6105–6116.
22. Zinszner, H., M. Kuroda, X. Wang, N. Batchvarova, R. T. Lightfoot, H. Remotti, J. L. Stevens, and D. Ron. 1998. CHOP is implicated in programmed cell death in response to impaired function of the endoplasmic reticulum. *Genes Dev.* **12:** 982–995.
23. Chen, X., J. Shen, and R. Prywes. 2002. The luminal domain of ATF6 senses endoplasmic reticulum (ER) stress and causes translocation of ATF6 from the ER to the Golgi. *J. Biol. Chem.* **277:** 13045–13052.
24. McCullough, K. D., J. L. Martindale, L. O. Klotz, T. Y. Aw, and N. J. Holbrook. 2001. Gadd153 sensitizes cells to endoplasmic reticulum stress by down-regulating Bcl2 and perturbing the cellular redox state. *Mol. Cell. Biol.* **21:** 1249–1259.
25. Ariyama, Y., H. Shimizu, T. Satoh, T. Tsuchiya, S. Okada, S. Oyadomari, and M. Mori. 2007. Chop-deficient mice showed increased adiposity but no glucose intolerance. *Obesity (Silver Spring).* **15:** 1647–1656.
26. Larade, K., Z. G. Jiang, A. Dejam, H. Zhu, and H. F. Bunn. 2007. The reductase NCB5OR is responsive to the redox status in beta-cells and is not involved in the ER stress response. *Biochem. J.* **404:** 467–476.
27. Kong, J. Y., and S. W. Rabkin. 2000. Palmitate-induced apoptosis in cardiomyocytes is mediated through alterations in mitochondria: prevention by cyclosporin A. *Biochim. Biophys. Acta.* **1485:** 45–55.
28. Sparagna, G. C., D. L. Hickson-Bick, L. M. Buja, and J. B. McMillin. 2000. A metabolic role for mitochondria in palmitate-induced cardiac myocyte apoptosis. *Am. J. Physiol. Heart Circ. Physiol.* **279:** H2124–H2132.
29. Ostrander, D. B., G. C. Sparagna, A. A. Amoscato, J. B. McMillin, and W. Dowhan. 2001. Decreased cardiolipin synthesis corresponds with cytochrome c release in palmitate-induced cardiomyocyte apoptosis. *J. Biol. Chem.* **276:** 38061–38067.
30. Listenberger, L. L., D. S. Ory, and J. E. Schaffer. 2001. Palmitate-induced apoptosis can occur through a ceramide-independent pathway. *J. Biol. Chem.* **276:** 14890–14895.
31. Song, B., D. Scheuner, D. Ron, S. Pennathur, and R. J. Kaufman. 2008. Chop deletion reduces oxidative stress, improves beta cell function, and promotes cell survival in multiple mouse models of diabetes. *J. Clin. Invest.* **118:** 3378–3389.
32. Larade, K., and H. F. Bunn. 2006. Promoter characterization and transcriptional regulation of Ncb5or, a novel reductase necessary for pancreatic beta-cell maintenance. *Biochim. Biophys. Acta.* **1759:** 257–262.
33. Wang, J., T. Takeuchi, S. Tanaka, S. K. Kubo, T. Kayo, D. Lu, K. Takata, A. Koizumi, and T. Izumi. 1999. A mutation in the insulin 2 gene induces diabetes with severe pancreatic beta-cell dysfunction in the Mody mouse. *J. Clin. Invest.* **103:** 27–37.
34. Oyadomari, S., E. Araki, and M. Mori. 2002. Endoplasmic reticulum stress-mediated apoptosis in pancreatic beta-cells. *Apoptosis.* **7:** 335–345.